3.2 Ozone Episodes in U.S.-Mexico Border Cities: Can Fusion of Satellite Information Improve the Accuracy of Predictions?

by

Chune Shi[1*] and H.J.S. Fernando

Department of Mechanical and Aerospace Engineering, Environment Fluid Dynamics Program, Arizona State University, Tempe, AZ, U.S.A.

Edmund Y.W. Seto

School of Public Health, University of California, Berkeley, CA, U.S.A

J. P. Muller

Mullard Space Science Laboratory, Dept. of Space and Climate Physics, University College London, Holmbury St Mary, Surrey, RH5 6NT, U.K.

1. Introduction

Chemical transport models (CTM) are usually evaluated using surface measurements, but increasing availability of space-borne remote sensing products offers a new and powerful tool to conduct such evaluations. Extensive geographical coverage and frequent observations of satellite measurements are particularly attractive in this context, as they minimize the necessity of interpolations among point surface measurements to compare with grid-averaged predictions. The study reported herein assesses the usefulness of tropospheric satellite data, in combination with those of surface monitoring networks, in evaluating ozone predictions of an air quality model. The motivation was to investigate the feasibility of utilizing satellite data to improve the prediction of the extent and severity of ozone pollution episodes in the Southwestern US.

The design of the study was centered on an ozone episode over South California, including US-Mexico boarder in San Diego, on August 8-10, 2006, recorded by the EPA's Air Quality System (AQS). The maximum 1-hr/8hr ozone concentration exceeded 120ppb/80ppb at several sites in San Diego. The episode was particularly striking on the 9th August, and hourly variation of ozone concentration (averaged over all observational sites on San Diego) is given in Figure 1.

2. Model configuration and data

2.1 Model configuration and input data

The simulations were conducted for the design days using the regional air quality model system of Models-3 (MM5v3.7/SMOKEv2.3/CMAQv4.5.1). The modeling domain was based on a Lambert projection centered at (97ºW, 40ºN), with horizontal grids of 36 × 36 km^2. The domain for MM5 covers the whole North American continent. For CMAQ and SMOKE runs, the domain covered the Southwestern U.S. with 74×70 horizontal grid cells. The troposphere from ground to 100hPa was divided into 29 model sigma layers, with 16 unevenly distributed vertical layers within the lower 2000m. The lowest layer near the ground was 7m, and highest resolution was maintained near the ground to better capture boundary-layer processes. The data for initialization and lateral boundary conditions were obtained from the NCEP/ETA model, NCEP global surface observations and NCEP global upper air observations. The National Emissions Inventory (NEI) databases of 2001 (for the US) and 1999 (MEXICO) were used for air quality simulations. For runs with default initial/boundary conditions (*default run*), the simulation began at 00GMT on August 4 and ended at 00GMT on August 11. The results of the first 4 days of simulations were discarded to account for the spin-up.

2.2 Data for Model Evaluations

The data for CMAQ evaluation consists of hourly ground level ozone concentrations from AQS repository, the level 2 products from TES (Beer et al., 2001) and the Atmospheric InfraRed Sounder (AIRS) (Aumann et al., 2003). There are more than 300 monitoring sites in the domain with the highest site densities in southern California.

3. Evaluations of CMAQ

3.1 Evaluations of CMAQ ground level ozone

The hourly observations are the averages of all sites in a cell, while the modeled values for each site are calculated by bilinear interpolation of the four surrounding cells. The modeled and observed hourly area-mean ozone concentrations are shown in Figure 1. The observed and simulated hourly area-mean values are highly correlated and the two maxima on August 9 are quite close, although large differences appear on August 8 and 10. The statistical results of all hourly data pairs at the nine sites in San Diego show that the model somewhat over-predicts multi-site ozone averages (MB=5.4ppb), with a medium index of agreement (0.77) and correlation coefficient (0.63); however, the simulated standard deviation (SD) is comparable to the observed and the root mean square deviation (RMSD) is lower than the observed SD. Overall, the statistical results indicate moderate but acceptable performance of Models-3 for surface ozone in San Diego.

Statistics between observations and simulations are calculated for all grids with monitors in the entire model domain (Table 1). The correlation coefficient for all hourly prediction-observation pairs is 0.66 for the entire model domain, consistent with that of San Diego. Overall, the diurnal ozone patterns were reproduced satisfactorily by CMAQ at most monitoring sites. 75% of the 200 cells with monitors have a correlation higher than 0.6, and more than 60% have NMB between -25% and 25%.

3.2. Evaluations of 3D CMAQ ozone for the middle to upper troposphere

The statistics between CMAQ and AIRS are given in Table 2, where, for example, the layer 850 hPa denotes the average between 850 hPa and 700 hPa. The results show that the *default run* simulated ozone concentrations reasonably well for most layers; however, both the correlation coefficient and the slope decrease with decreasing pressure (850 hPa to 400 hPa) and the simulated concentrations are lower than those of AIRS at all layers by 20%~30%. The correlation coefficient reaches its minimum at 400 hPa, and then increases with decreasing pressure while the slope maintains a low value (<0.1).

4. Efficacy of TES data as initial/boundary conditions for CMAQ

The TES data from August 4 and 8, 2006 were first filtered to extract daytime data for the overpass time for North America (~1 PM LT or 20:00 GMT). The filtered data were mapped to the model grids using the griddatan function in MATLAB. The TES data of August 4 and August 8 provide boundary conditions for August 4-7 and August 8-10, respectively (*test run*).

The footprints of two TES traverses in the model domain (identified “A” and “B” for different dates) on August 9 are shown in Figure 2. The crosses are the locations and the numbers are satellite overpass times, assigned with a lower case letter to stamp each satellite pixel. Footprint A corresponds to local nighttime and footprint B to local daytime.

4.1. Ground level ozone

Average statistics between ozone observations and the *test run* ozone concentrations are included in Table 1. The differences between the two simulations are

negligible for most of the statistical measures. For the ozone episode area of San Diego, the correlation coefficient for all hourly prediction-observation pairs is 0.64, which is close to that obtained in the default run.

4.2. Tropospheric ozone profiles

CMAQ simulated ozone concentrations were binned to the TES vertical layers by assuming that ozone is evenly distributed in a model grid. Figures 3 and 4 display comparisons of TES-measured and CMAQ-simulated ozone profiles in default and test runs over each TES pixel at the footprint in Figure 2.

The TES observed ozone profiles varied with the latitude. During the night (Figure 3), ozone increases with height in the lower troposphere at different rates and then increases or decreases slowly with height or remains unchanged in the middle troposphere (700~400 hPa), with some profiles having a minimum at 300 hPa. The ozone concentration then begins to increase quickly at most pixels, with the rate of increase growing with increasing latitude. A(d) and A(h), however, are exceptions with pronounced maxima over 100 ppb at 700 hPa. Pixel A(d) is located close to metropolitan Los Angeles and perhaps is acting as a “nocturnal ozone reservoir” as a result of ozone lofting during the daytime (Lee et al., 2003). At noon, the ozone concentrations change little below 600 hPa at all pixels (Figure. 4) but vary with latitude above this altitude.

In the *default run*, over both tracks, the simulated ozone profile shapes are quite similar at different locations for heights above 600 hPa. The ozone concentrations of the *default run* are ~ 70 ppb, much the same as the default no-flux top boundary concentrations, which are much lower than the TES observations in the upper troposphere for most pixels. Nevertheless, the ozone profile shapes from the *test run* and the TES-measurements showed better agreement in the upper troposphere.

In the lower troposphere, below 700 hPa, ozone profiles from the two runs are similar, but generally profiles from the *test run* are closer to the observations. Also note that in the lower troposphere there are some ozone maxima in TES observations close to the dense emission areas of Los Angeles and San Francisco ((d) in Figure 3), while in both simulations such distinct maxima were not captured. This may be due to the lower resolution of the simulations (36 km horizontal, with varying vertical resolution) compared to TES observations (about 5 km in the horizontal and 500 m in the vertical). Also note that the zero-gradient (Neumann) boundary condition is applied in CMAQ, thus weakening the boundary influence.

As noted, when IC/BC for CMAQ is provided by TES data, improvement is noted in the predicted profile for the upper troposphere (500 ~ 200 hPa) at most pixels when compared with the subsequent TES observations. The statistics between TES measured and CMAQ simulated ozone concentrations in the upper troposphere (500 ~ 200 hPa) over both A and B columns are in Table 3. The correlation/slope changed from 0.15/0.03 (insignificant at 99%) in the *default run* to 0.6/0.52 (significant at 99%) for the *test run*. Statistics for the lower troposphere, however, shows weak correlations with TES data for both *default* and *test runs* and are not shown here.

Based on the analysis above, the default lateral and constant top boundary ozone concentrations are found to be inadequate to reproduce measured variability of ozone with latitude and height in the troposphere.

4.3. 3D CMAQ ozone concentrations in the middle to upper troposphere (850 -200 hPa)

For the design days, only three TES and AIRS pixel pairs are available for the same model grid at the same time. From the profiles in Figure 3, it can be seen that the AIRS data do not match the TES data well. For pixels (c) and (f), AIRS profiles are closer to the *test run* than to the TES observations, pointing to the need for reconciliation between data from different

satellites.

The statistics between AIRS measured and CMAQ simulated ozone concentrations (*default* and *test runs*) at each layer in the middle to upper troposphere are in Table 2. Both runs show the worst correlation at 400 hPa. At 850 hPa, the *test run* is a bit worse than the *default run* in both correlation and slope. At 700 hPa and 600 hPa, the *test run* has lower correlations and higher slopes than the *default run*, but the differences are small. In addition, both the mean bias (MB) and NMB between the *test run* and AIRS are smaller than those between the *default run* and AIRS. Consequently, the performance of the *test run* is comparable to that of the *default run* in the middle troposphere. However, in the upper troposphere (above 500 hPa), the *test* run is far superior to the *default run* in both the correlation and the slope, and the MB and NMB changed from negative to positive. Since AIRS ozone profiles are of high quality in the upper troposphere (Aumann et al., 2003; Bian et al., 2007), and AIRS ozone concentrations are about -2~-30% lower than ozonesonde ozone concentrations between 400 and 150 hPa in the summer (Bian et al., 2007), we conclude that the TES-based IC/BC indeed improves the CMAQ performance in the upper troposphere.

5. Summary and conclusions

In this work we presented the evaluations of two CMAQ simulations by ground level observations and satellite observed 3D tropospheric ozone concentrations. The main aim of this study was to investigate whether the ozone predictions of a 3D air quality modeling system can be improved by utilizing satellite data to provide IC/BC.

CMAQ showed moderate but acceptable performance for ground level ozone in the episode area. The modeled ozone concentrations correlated well with AIRS data (r= 0.43 ~ 0.53) with normalized mean biases of about -20% in different layers of the middle troposphere. The correlations decreased in the upper troposphere with very low slopes.

Attempts to improve the predictions of surface ozone using TES data as IC/BC were not successful. The same was true for ozone concentrations in the lower troposphere (TES) and middle troposphere (AIRS). The use of TES-based IC/BC, however, did produce a significant improvement in the correlation coefficient between CMAQ predictions and TES/AIRS observations for upper-tropospheric ozone. The inability of satellite data ingestion to improve surface ozone prediction can be attributed to the dominance of local surface emissions in ozone chemistry, rather than the advection of ozone into the domain and entrainment from the lower stratosphere, which is more accurately represented by employing TES-based IC/BC (Hocking et al., 2007). As such, TES-based simulations can significantly improve CMAQ predictions for the upper troposphere.

Acknowledgement

The support of Advanced Monitoring Initiative of the U.S. EPA is greatly acknowledged. During the project period, the authors were also supported by the National Science Foundation (ATM), Arizona Department of Environmental Quality, the Science Foundation of Arizona and Vice President for Research at ASU. The AIRS 3D ozone data provided by the website hosted by NASA Goddard Earth Sciences Data and Information Services Center (GES DISC), and TES ozone profile data provided by the website of Atmospheric Science Data Center. We would like to thank all AMI collaborators and facilitators, especially Vance Fong and Rick van Schoik, for useful discussions and Peter Hyde for valuable comments.

References

Aumann, H.H., Chahine, M.T., Gautier, C., et al., 2003. AIRS/AMSU/HSB on the Aqua Mission: Design, Science Objectives, Data products, and Processing System.

IEEE Transaction, Geoscience and Remote Sensing 41(2), 253-264.

Beer, R., Glavich, T.A., Rider, D.M., 2001. Tropospheric Emission Spectrometer for the Earth Observing System's AURA satellite. Applied Optics 40(15), 2356-2367.

Bian, J., Gettelman, A., Chen, H., Pan, L.L., 2007. Validation of satellite ozone profile retrievals using Beijing ozonesonde data. Journal of Geophysical Research 112: D06305, doi:10.1029/2006JD007502.

Hocking, W.K., Carey-Smith, T., Tarasick, D.W, et al., 2007. Detection of stratospheric ozone intrusions by windprofiler radar. Nature 450(8), 281-284.

Lee, S.M., Fernando, H.J.S., Princevac, M., et al., 2003. Transport and diffusion of ozone in the nocturnal and morning PBL of the Phoenix valley. Environmental Fluid Mechanics 3, 331-362.

Table 1: Statistical results of ground level ozone between AQS data and CMAQ predictions for the entire model domain

Variables	r	Slope	NMB %	MB ppb	GridNO r>0.6	GridNO |nmb|<25%	TotalGrid
Default run	0.70	0.51	6.4	0.0	149	127	200
Test run	0.69	0.54	14.3	2.9	145	131	200

Reference: the linear equation is Y=A×X + B, where X, Y, A and B refer to observed ozone, modeled ozone, slope and intercept, respectively. NMB (normalized mean bias); MB(mean bias); GridNO (grid number). Same in Table 2, 3.

Table 2 Statistical results between AIRS and CMAQ for each layer for the time period of 8-11 August, 2006

Pressure (hPa)	Default run					Test run					Mean AIRS (ppb)	Total Sample
	r	slope	MB (mb)	NMB (%)	Mean (ppb)	r	slope	MB (ppb)	NMB (%)	Mean (ppb)		
850	0.53	0.52	-9.8	-17.9	44.7	0.35	0.43	-5.2	-9.6	49.2	54.5	6080
700	0.47	0.45	-13.8	-22.4	47.9	0.42	0.60	-6.2	-10.1	55.5	61.7	6312
600	0.43	0.33	-16.6	-24.2	51.9	0.38	0.54	-3.9	-5.7	64.7	68.6	6312
500	0.38	0.21	-15.9	-21.5	58.2	0.40	0.56	5.4	7.2	79.5	74.2	6312
400	0.12	0.04	-15.3	-19.2	64.6	0.22	0.32	13.2	16.6	93.1	79.9	6312
300	0.24	0.05	-18.5	-21.7	66.7	0.26	0.45	34.5	40.5	119.8	85.3	6312
250	0.41	0.04	-30.6	-31.1	67.7	0.74	0.64	26.3	26.8	124.6	98.3	6312

Table 3 Statistical results between CMAQ and TES in the upper troposphere

Variables	Default run	Test run
r	0.15	0.60
slope	0.03	0.52
MB	-15.17	24.12
NMB	-19.26	30.63
Mean	63.58	102.86
Total samples	171	

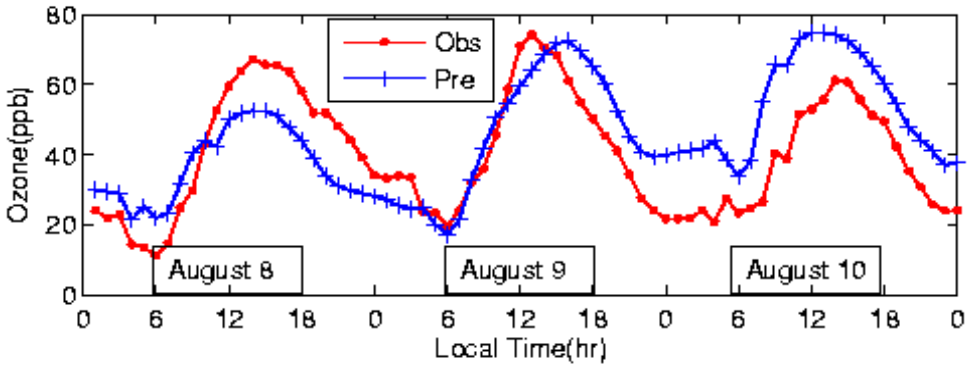

Fig. 1. Hourly variation of area-averaged ozone concentration in San Diego. (Obs-Observation; Pre-Prediction)

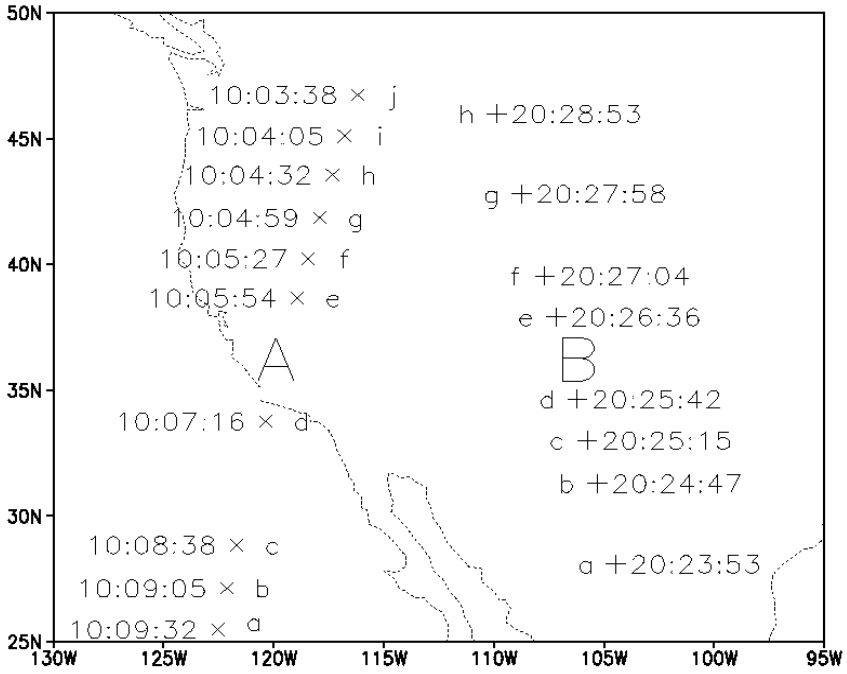

Fig. 2. The location of TES observations, with the numbers showing the measurement time in GMT; Symbols A and B denote footprints. The A footprint with its pixels a-j was taken on August 9, 2006 (Figure 3). The B footprint was taken on August 8 (Figure 4).

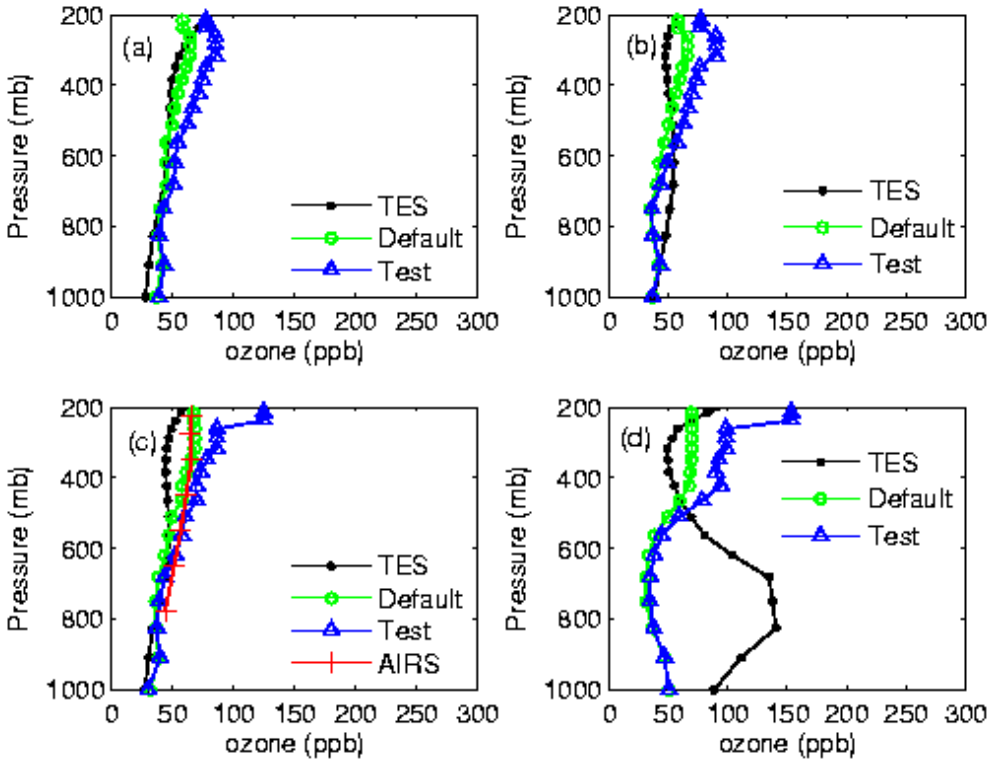

Fig. 3. Comparison of tropospheric ozone profiles at pixels (a)-(j) of column A in Fig. 2 from TES and AIRS observations with the corresponding CMAQ profiles using IC/BC from default values ("Default") and from TES observations ("Test").

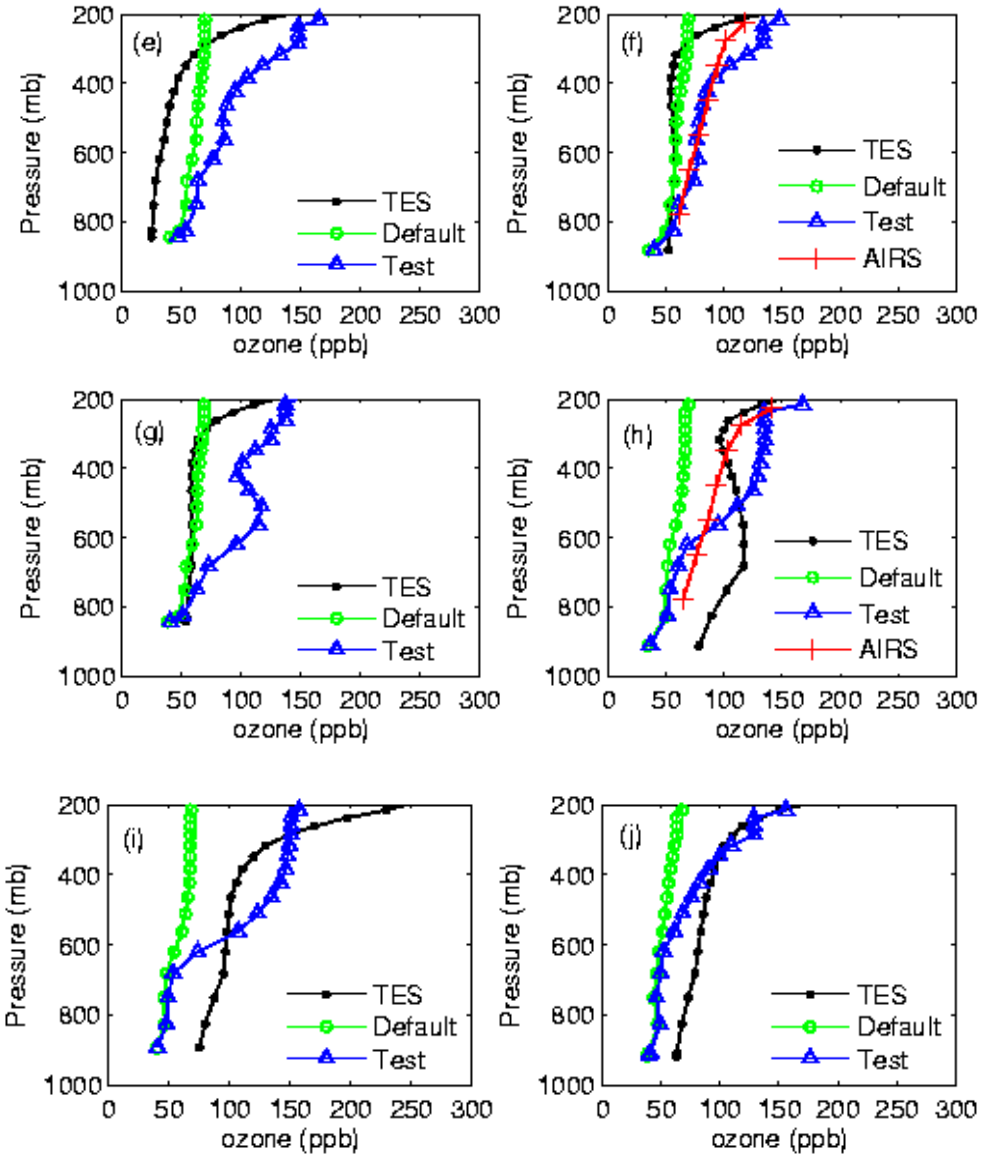

Fig. 3. Continued

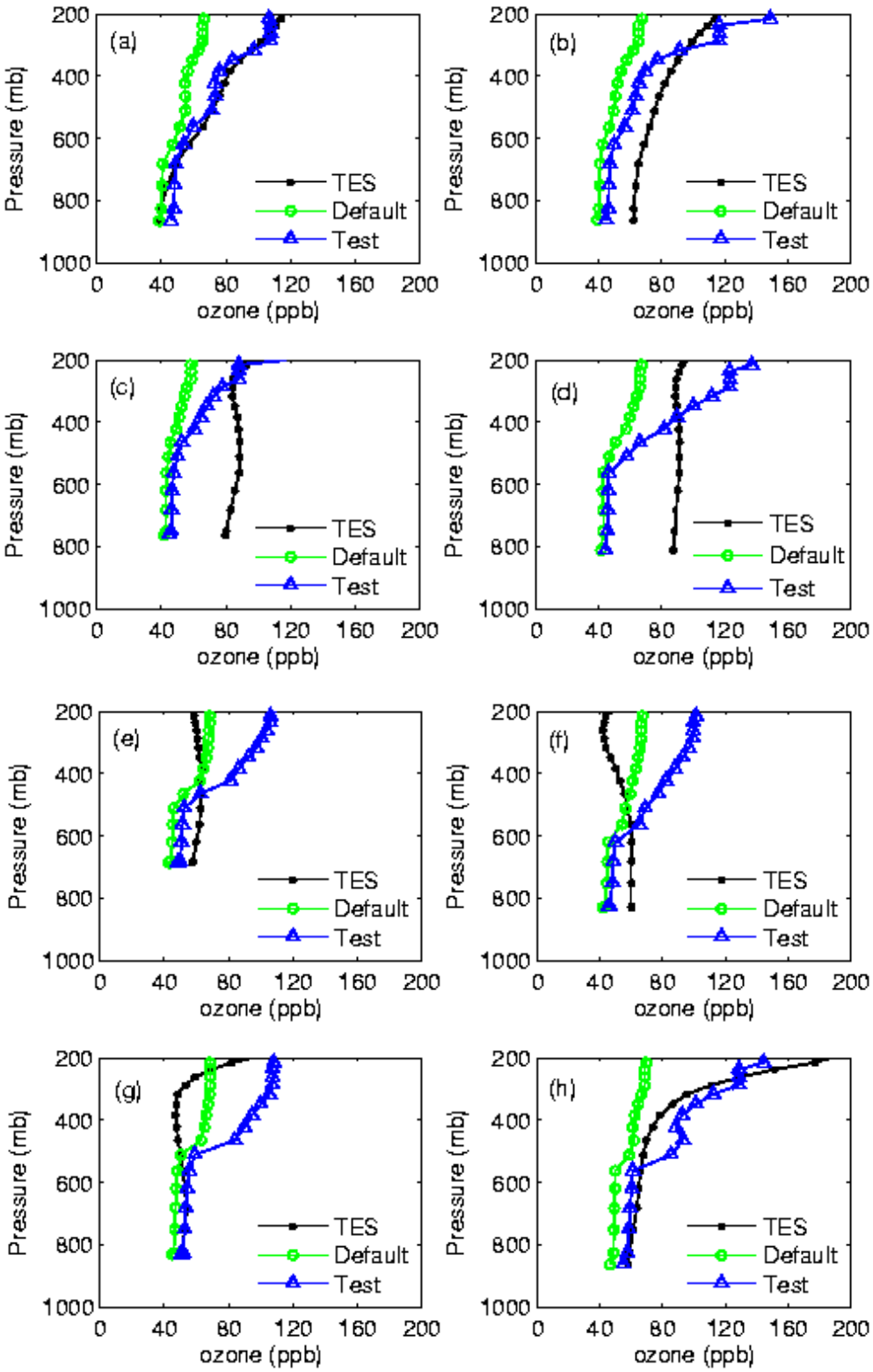

Fig. 4. Comparison of tropospheric ozone profiles at pixels (a)-(j) of column B in Fig. 5 from TES observations with the corresponding CMAQ profiles using IC/BC from default values ("Default") and from TES observations ("Test").